Excimer Laser Drilling of Polymers

ABSTRACT

Laser micro-drilling technology plays a more and more important role in industry, especially in the fabrication of multi-layer electronic packages. In such applications, non-metals are often used as insulators, in which via holes are formed to provide vertical interconnections for densely packed three dimensional wiring networks. Mechanical punch tools have been the primary means to form holes in ceramic sheets and in polymer boards since the 1970's. As the cost of fabricating punch heads increases drastically and the demand for quick turn around part build becomes more routine, flexible via forming technologies, such as laser drilling, have become more prevalent. In laser drilling, CO_2, Nd:YAG, and excimer lasers are often used. Their drilling capabilities, drilling mechanisms, and hole qualities are different because of the different laser beam characteristics such as wavelength and beam energy distribution. In this paper, the mechanisms of laser drilling are briefly reviewed. The results of the experiments on excimer laser drilling of two types of polymer: polyimide and polyethylene terephthalate, are reported. It is found that the etch rate increases with increase of fluence, and the wall angle of drilled holes is dependent on the fluence. The material removal by a laser pulse is highly controllable. There exists an optimal fluence range to obtain clean and smooth edges of quality holes for a given material at a given laser wavelength.

Keywords: excimer laser, laser drilling, laser etching, laser micro-machining, polymers.

1. INTRODUCTION

Laser drilling of various materials (e.g. metals, non-metals, plastic, and ceramics) has been an accepted production-line facility for many years[1]. Of all the laser drilling applications, via hole formation plays an important role in electronic packaging processing. As the packaging wiring density and complexity increases, additional and more stringent demands are put on the via formation technology (e.g. tighter dimensional control, higher via positional accuracy, etc.). The push for miniaturisation demands vias to go below 50 μm feature size[2]. Over the years, several via formation technologies have been developed and implemented for manufacturing high performance electronic packages. They range from the traditional mechanical punch to the state-of-the-art directed energy technologies such as laser and electron beam machining. Of all the via formation technologies, laser drilling technology is considered one of the better techniques to meet the requirements due to the small beam spot, accurate drilling depth control and minimum heat affected zone.

Among the lasers used for micro-drilling, three key types of lasers are CO_2, Nd:YAG and excimer lasers. The high degree of precision in the excimer laser processing and the absence of damage to the surrounding materials have been reported[3]. In this paper, experimental results of excimer laser micro-drilling of polymers will be presented.

2. MECHANISM OF LASER DRILLING

The dominant physical process involved in laser drilling can be thermal or photochemical, depending largely on the laser wavelength. Shorter wavelengths (in the UV range) have higher photon energy leading to photo-chemical reactions. Longer wavelengths in the infrared range have lower photon energy leading to thermal reactions.

2.1. Material removal mechanism (thermal processes)

A variety of physical and chemical processes may take place during CO_2 and Nd:YAG laser drilling, including heating, melting, vaporisation, and molten material expulsion. Two of these processes, i.e. vaporisation and molten expulsion, result in removal of material, i.e., drilling. The material removal mechanism and rate depend on the incident laser power level, the thermal properties of the material, and whether or not an assist gas jet is used[4].

2.2. Laser ablation characteristics (photochemical processes)

For excimer laser drilling, the mechanism is different from the thermal processes prevalent in CO_2 and YAG laser drilling. It is generally accepted that the removal of materials, e.g. polyimide, is through ablation, where the absorbed UV photons directly break the chemical bonds[5]. Hence, if sufficient photons are incident on a thin layer of material in a short time interval, a pressure increase is generated due to the rapid formation of lower molecular weight components. The process is essentially photochemical in nature leading to little thermal heating.

When a laser pulse from an excimer laser impinges on a polymer surface (as shown in Figure 1), the penetration of the radiation through the solid follows a simple relation which is known as Beer's law[5]

$$I_t = I_0 \cdot 10^{-\alpha l} \tag{1}$$

where I_0 and I_t are the intensities of the beam before and after transmission through a slice of material of thickness l, and α, the absorption coefficient, is a characteristic property of the material. If the fluence F (or energy density) of the laser beam at the workpiece exceeds a certain threshold value, F_0, then a depth, l_f of the material is ablated by the pulse. The next pulse will go through virgin material underlying it till the depth of the hole is reached.

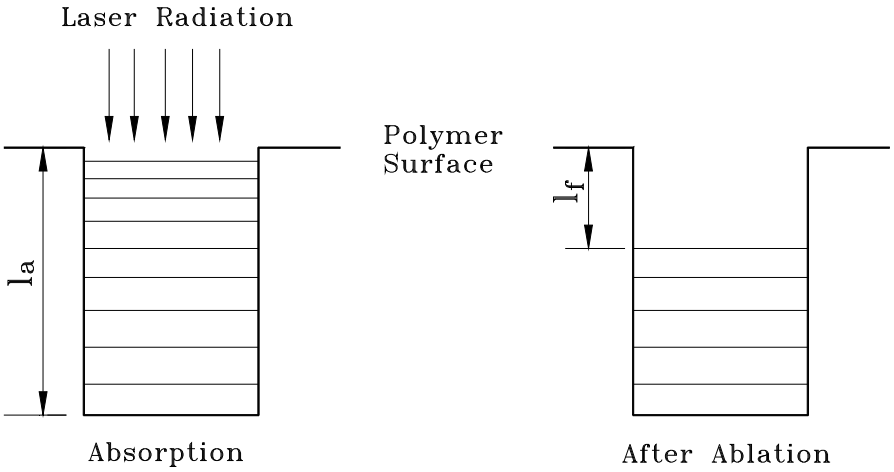

Fig. 1 Schematic representation of impact of laser pulse on polymer surface

Experiments have shown that all absorbed energy appears as heat below threshold fluence F_0, and the absorbed fluence needed to produce ablation, expressed as the product of the threshold fluence F_0 and the (effective) UV absorption coefficient α, is approximately constant for a given polymer[6, 7]. Above the ablation threshold, the etch depth per pulse (or so-called etch rate), l_f, can be approximated by[8]

$$l_f = \frac{1}{\alpha} \ln\left(\frac{F}{F_0}\right) \tag{2}$$

3. EXPERIMENTAL SET-UP

The excimer laser processing system is supplied by Exitech Limited. The laser used in this system is Model LPX 220i of Lambda Physik. The laser beam coming out from the laser generator goes through a beam homogenisation system and an optical projector unit. A mask is imaged on the workpiece on an X-Y-Z table. The table is driven by a CNC controller. A laser profiler is used to analyse beam energy distributions and a CCD camera is used to locate the workpiece and monitor the machining processes. The typical laser parameters used in the experiments are:

⇒	Wavelength	:	248 nm
⇒	Maximum pulse energy	:	300 mJ
⇒	Maximum pulse repetition rate	:	200 Hz
⇒	Nominal pulse duration	:	20 ns
⇒	Pulse-to-pulse stability	:	± 5 %
⇒	Beam dimension	:	(5 to 12) × 23 mm
⇒	Beam divergence	:	1×3 mrad

Figure 2 shows a schematic diagram of the optical mask projector. Such a layout is commonly used for excimer laser micromachining or etching. The condenser lens situated just before the mask focuses the laser beam into the entrance pupil of the projection lens. An image of the mask (or a variable aperture) is projected through high resolution lenses onto the workpiece.

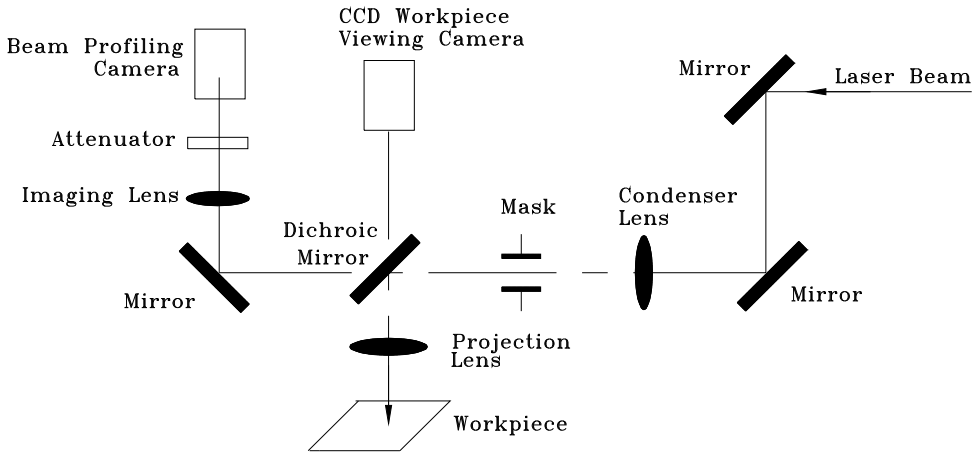

Fig. 2 Schematic diagram of the mask projector

Figure 3 shows the geometrical layout of mask projection. The mask is a rectangle of size $d \times h$, and the workpiece is located at L away from the projection lens. The fluence at the workpiece surface, E_d, is then given by[9]

$$E_d = \frac{\eta f^2 E_{out}}{(L-f)^2 hd} \tag{3}$$

where E_{out} is the uniform laser energy incident on the mask window, and η is the energy transmittance of the projection lens. If the workpiece surface is at the image position of the mask, that is,

$$L = l' = \frac{lf}{l-f} = \frac{l}{\beta} \tag{4}$$

where β is the de-magnification ratio of the lens and l is the distance between the mask and the projection lens, Equation (3) becomes

$$E_d = \frac{\eta \beta^2 E_{out}}{hd} \tag{5}$$

In our applications, the magnification ratios of the lens are always given and the via hole micromachining is done at the image position of the mask.

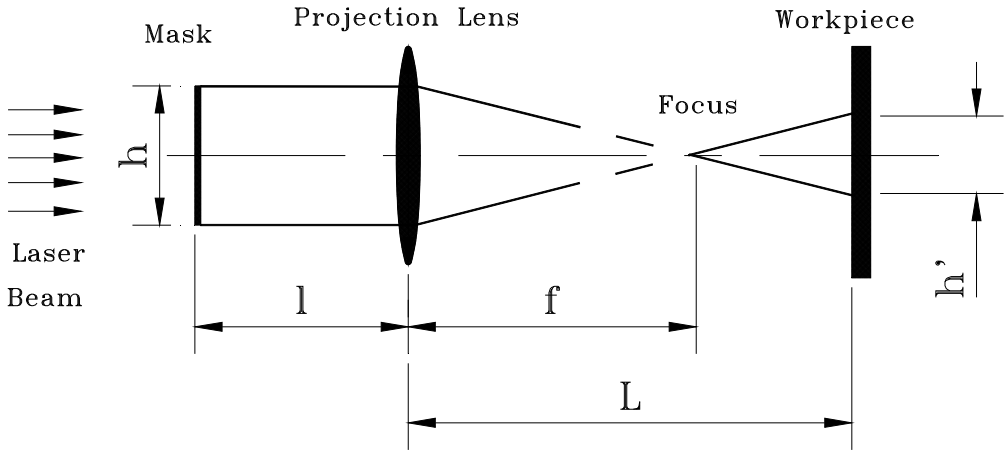

Fig. 3 Geometrical layout for mask projection

After excimer laser drilling, the sample is cleaned in an ultrasonic tank for 30 minutes at 50 ^{o}C, which removes most of the loose particles. It is then sent for plasma cleaning to remove the fine carbon residues. The plasma cleaning parameters are:

⇒ gas : 70% Ar + 30% O_2
⇒ pressure : 8.5 m.torr
⇒ power : 60 W
⇒ temperature : < 45 ^{o}C
⇒ time duration : 12 minutes

4. MICRO-DRILLING OF POLYIMIDE

The thickness of the polyimide specimen is 0.050 mm used typically in multi-layer hybrid circuits and other areas of VLSI technologies. The sizes of the etched holes range from 94.5 μm to 107.5 μm.

4.1. Effect of fluence on etch rate

A focusing lens with a demagnification ratio of 15× and a numerical aperture of 0.1 is used. The relationship between etch rate and fluence is shown in Figure 4. The etch rate increases with increasing fluence, whose trend agrees with Equation (2). Using Equation (2), it can be estimated that α = 4.55 μm^{-1} and F_0 = 0.277 J/cm^2. A more accurate estimation of the absorption coefficient can be obtained in consideration of the absorption coefficient of the ablation plume produced during the laser ablation process[8].

It should be noted that the etch rate is calculated by taking the average of a few hundred pulses at the given energy fluence. Individual pulses may cause slightly different amounts of material removal due to energy fluctuations of ±5%. However, the effect of these fluctuations is insignificant for the multi-pulse drilling process.

Clean and smooth edges are obtained with energy densities below 2.7 J/cm^2 (see Figure 5), while higher energies lead to the formation of some structures or debris at the top surfaces of the edges (see Figure 6). One possible reason is, at high fluence, the process no longer remains purely photochemical in nature and significant thermal degradation can occur[11].

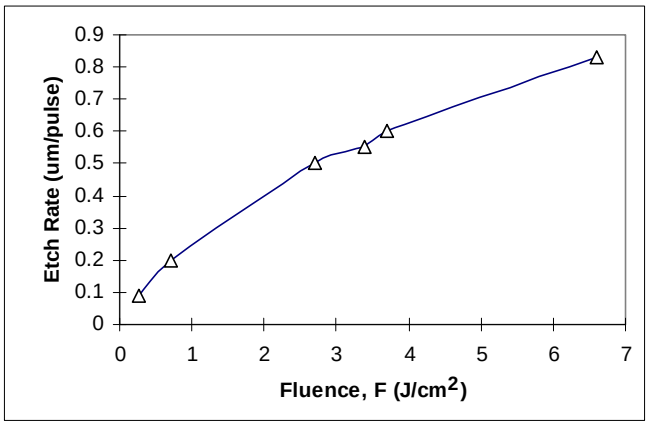

Fig. 4 Etch rate vs. fluence for polyimide

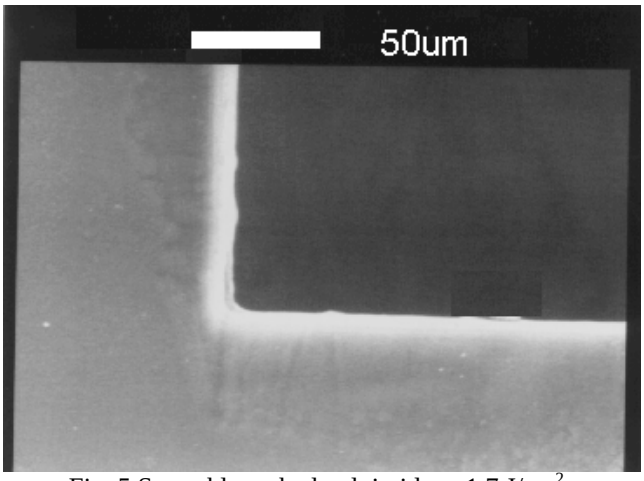

Fig. 5 Smoothly etched polyimide at 1.7 J/cm^2

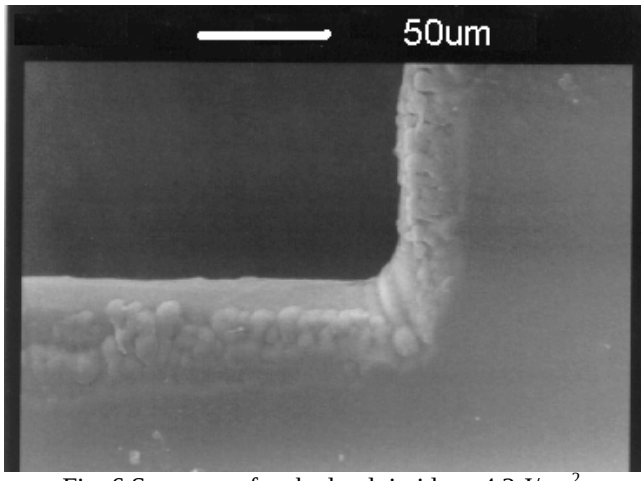

Fig. 6 Structure of etched polyimide at 4.2 J/cm^2

4.2. Effect of fluence on wall angle

Figure 7 shows the relationship between the wall angle and the fluence, where the demagnification ratio is 36× and the numerical aperture of the lens is 0.5. It should be noted that the wall angle (θ) is calculated based on the top and bottom hole diameters, and the thickness (τ) of the materials:

$$\theta = \frac{180}{\pi} \cdot \frac{1}{2} \cdot \frac{\phi_{top} - \phi_{bottom}}{\tau} \text{ (degrees)} \qquad (6)$$

where ϕ_{top} and ϕ_{bottom} are the hole diameters at the top and at the bottom of the workpiece drilled, respectively.

It is clear from Figure 7 that the wall angle decreases with an increase of energy fluence. This is probably due to diffractive effects at the edge of the pattern that produces lower fluences and etch rates in the region. Once initiated the taper is favoured by the lower fluence experienced at the wall for non-normal angles of incidence of the beam[10]. Another probable cause is spherical aberration of the uncorrected but cheaper lenses used in the study.

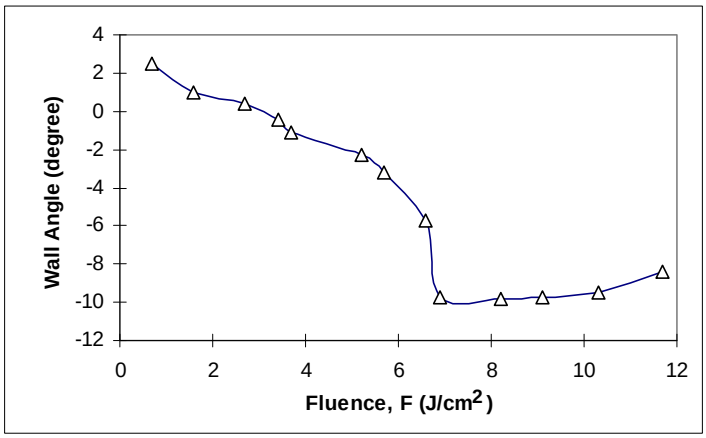

Fig. 7 Wall angle vs. fluence

Further increase in the beam fluence causes the angle to cross the zero point and becomes a negative value. The phenomenon can be explained in two aspects. First, the increased energy is larger than the energy threshold even with diffractive effects at the edges, and secondly, the beam size is enlarged greatly due to the defocusing effect. However, this phenomenon is not observed when using lower NA lenses (e.g. when using the 4× lens with *NA = 0.1*), which is probably due to the longer depth of focus for lower NA lenses (*depth of focus = 0.8 λ/NA*^{2})[10].

A tapered hole drilled at 1 J/cm^2 is shown in Figure 8 (bigger on the top surface). At a higher energy of 5.7 J/cm^2, shown as Figure 9, the hole diameter at the bottom surface is bigger than that at the top due to the defocusing effect. However, to obtain a more accurate wall angle, the hole needs to be cross-sectioned. These results show that different types of holes can be produced using different lenses and laser energy densities. That means that the wall angles are selectable.

An aspect ratio (ζ) is defined as the ratio of the hole diameter (ϕ) to the hole depth (d), that is $\zeta = \phi/d$. Figure 10 shows a hole with an aspect ratio of 1:10, which was the best achievable for the current set-up. Here the de-magnification of the projection lens with NA of 0.4 is 25×, the fluence is 9.2 J/cm^2.

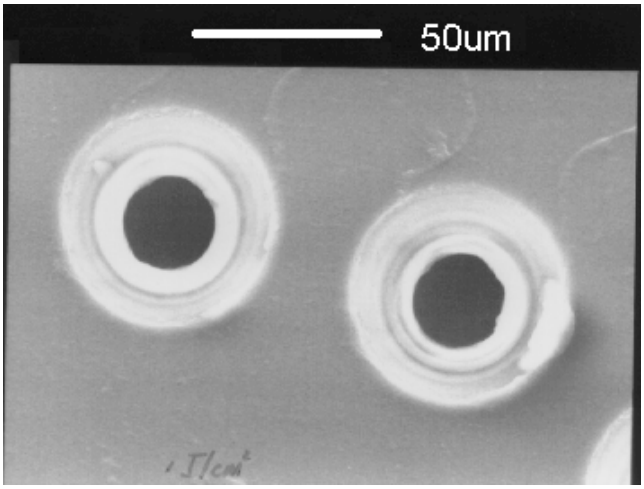

Fig. 8 A hole with a bigger diameter on the top surface) (top view)

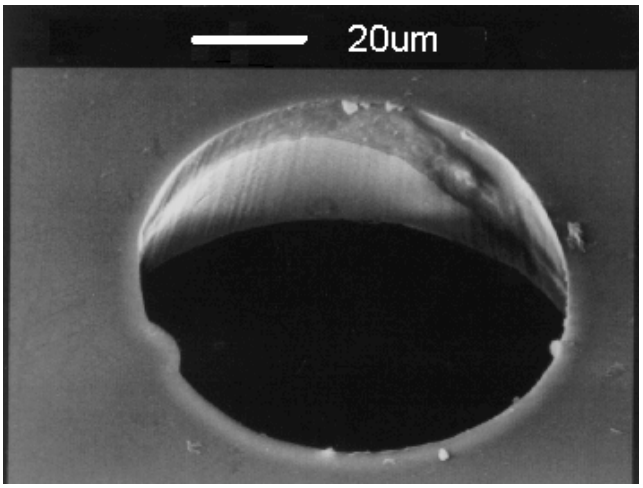

Fig. 9 A hole with a bigger diameter on the bottom surface (Photo tilted @ 43^o)

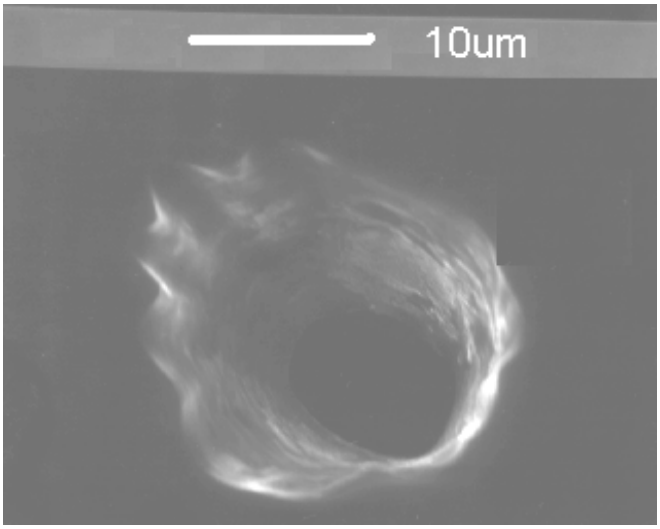

Fig. 10 A hole with an aspect ratio of 1:10 for polyimide of 0.05 mm thickness

5. MICRO-DRILLING OF POLYETHYLENE TEREPHTHALATE (PETP)

A projection lens with a de-magnification ratio of 15× and a numerical aperture of 0.28 is used. The thickness of the material is 75 μm. The material is the most important material for blow moulded components (bottles) and widely used as electrical insulation and printing sheets.

5.1. Effect of fluence on etch rate

Figure 11 shows the etch rate as a function of fluence. The etch rate increases fairly linearly with increasing fluence. Using Equation (2), it can be estimated that $\alpha = 3.99\ \mu m^{-1}$ and $F_0 = 0.203\ J/cm^2$.

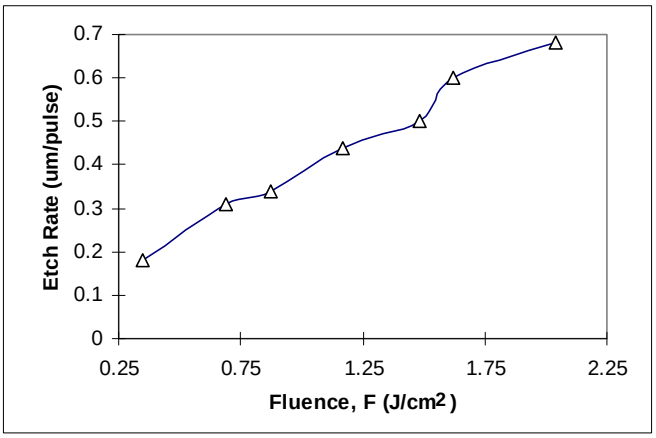

Fig. 11 Etch rate vs. fluence for PETP

Clean and smooth edges are obtained at the fluence of 0.36 J/cm^2 as shown in Figure 12(a). However, surface structures appeared at high energy densities as illustrated in Figure 12(b). This is probably due to the thermal melting effect or debris at these high energy densities.

As another example, a shallow etch pattern is produced as shown in Figure 13, where the fluence is 2.34 J/cm^2 with 100 pulses. Fine structures were observed despite uniform laser beam intensity as given in the energy profile plot shown in Figure 14.

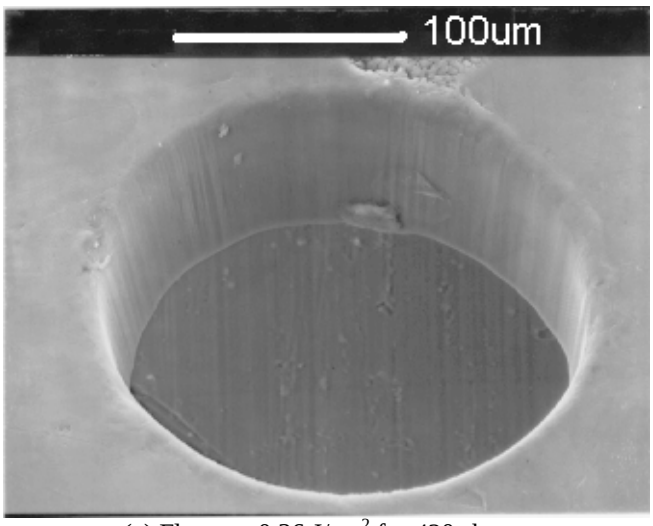

(a) Fluence: 0.36 J/cm^2 for 420 shots

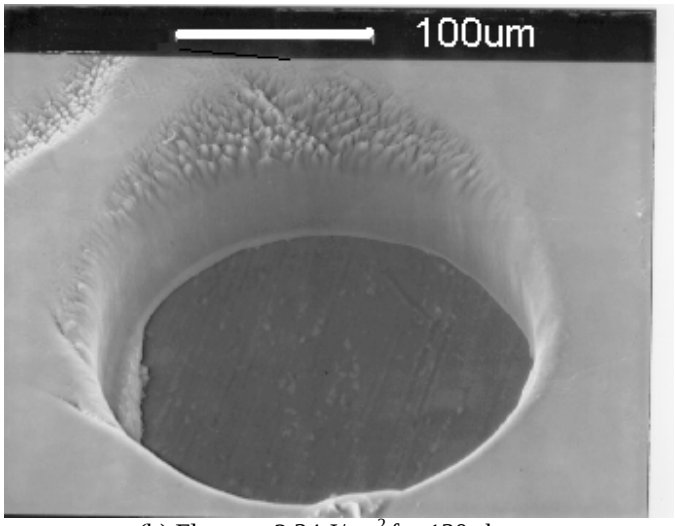

(b) Fluence: 2.34 J/cm^2 for 130 shots

Fig. 12 Photos of etched PETP sheets

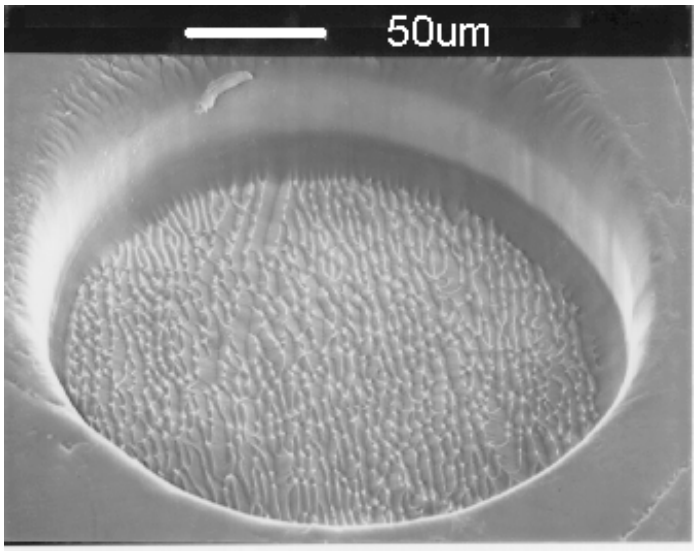

Fig. 13 Shallow crater with fine structures produced in PETP (2.34 J/cm^2 for 100 pulses)

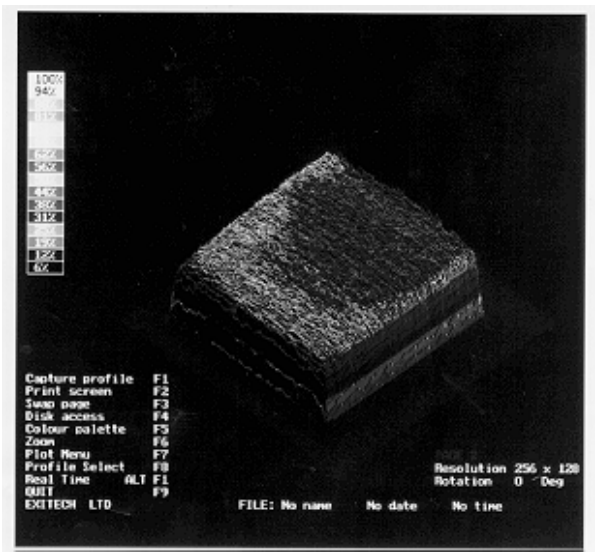

Fig. 14 Uniform laser energy distribution

5.2. Effect of fluence on wall angle

Figure 15 shows the wall angle as a function of fluence. It is clear that the wall angles decrease with increasing energy densities. There is no negative value of the wall angles. The reasons are due to a lower numerical aperture and a lower fluence used in the experiments.

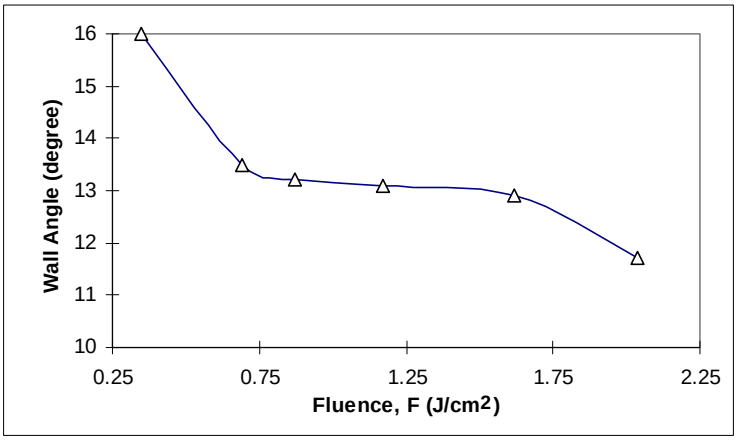

Fig. 15 Wall angle vs. fluence for PETP

6. CONCLUSIONS

In excimer laser drilling of polymers such as polyimide and PETP, the etch rate increases with increasing fluence. However the wall angle does not show any linear relations with the fluence, but is controllable. A hole with an aspect ratio of 1:10 is obtained. The material removal by a laser pulse is highly controllable and blind holes can easily be produced. This characteristic is specially suitable for some applications such as via formation and the scribing of indium titanium oxide films. There exists an optimal fluence range to obtain clean and smooth hole edges for a given material at a given laser wavelength. In this study, it has been determined that optimal energy densities are 1.7 J/cm^2 and 0.36 J/cm^2 for polyimide and PETP respectively.

ACKNOWLEDGEMENTS

The authors gratefully acknowledge the technical support of the Advanced Machining Group of Gintic Institute of Manufacturing Technology.

REFERENCES

1. I. W. Boyd, *Laser Processing of Thin Films and Micro-structures: Oxidation, Deposition, and Etching of Insulators*, Springer-Verlag, Berlin, 1987.
2. J. Tourne, "Laser via technologies for high density MCM-L fabrication", *Proceedings of 1995 International Conference on Multichip Modules (SPIE Vol. 2575)*, Reston VA, USA, pp. 71-76, 1995.
3. D. Poulin, J. Reid, and T. Znotins, "Materials processing with excimer lasers", *International Congress on Applications of Lasers and Electro-Optics (ICALEO)*, San Diego, CA, Nov. 1987.
4. R. S. Patel and M. Q. Brewster, "Gas-assisted laser-metal drilling: experimental results", *Journal of Thermophysics and Heat Transfer*, Vol. 5, No. 1, pp. 26-31, 1991.
5. R. Srinivasan, "Ablation of polymers and biological tissue by ultraviolet lasers", *Science*, Vol. 234, pp. 559-565, 1986
6. P. E. Dyer and J. Sidhu, "Excimer laser ablation and thermal coupling efficiency to polymer films", *Journal of Applied Physics*, Vol. 57, No. 4, pp. 1420-1422, 1985.
7. G. M. Davis and M. C. Gower, "Wavelength dependence of the excimer laser etching characteristics of a polymeric resist", *Applied Physics Letters*, Vol. 50, No. 18, pp. 1286-1288, 1987.
8. P. E. Dyer, "Laser ablation of polymers", in *Photochemical Processing of Electronic Materials*, edited by I. W. Boyd and R. B. Jackman, pp. 360-385, Academic Press Limited, London, 1992.
9. Y. H. Chen, Z. H. Tang, and J. L. Qiu, "Optical parameters computation for CO_2 laser marking system", *Laser Technology*, Vol. 18, No. 1, pp. 38-41, 1994 (in Chinese).
10. R. C. Crafer and P. J. Oakley, *Laser Processing in Manufacturing*, pp. 189-272, Chapman & Hall, London, 1993.
11. Exitech Limited, *EU 205 Project: Applications of High Power Excimer Lasers*, Phase I, 1989